1 **The loss of the PDIM/PGL virulence lipids causes differential secretion of ESX-1 sub-**

2 **strates in *Mycobacterium marinum***

3

4 Running Title: Virulence Lipids are Essential for Protein Secretion

5

6 Bradley S. Jones[*1,2], Daniel D. Hu[*3], Kathleen R. Nicholson[1,4], Rachel M. Cronin[1], Matthew M

7 Champion[2, 3#], and Patricia A. Champion[1,2#]

8 [1]Department of Biological Sciences, [2]Eck Institute for Global Health, [3]Department of Chemistry

9 and Biochemistry, University of Notre Dame, Notre Dame, Indiana, 46556

10 [4]Current Address: Department of Microbiology-Immunology, Feinberg School of Medicine,

11 Northwestern University, Chicago, Illinois, 60611

12 [#]Please address correspondence to pchampio@nd.edu or mchampio@nd.edu

13 [*]Authors contributed equally to this work.

14 **Abstract:**

15 The mycobacterial cell envelope is a major virulence determinant in pathogenic mycobacteria.

16 Specific outer lipids play roles in pathogenesis, modulating the immune system and promoting

17 the secretion of virulence factors. ESX-1 (ESAT-6 system-1) is a conserved protein secretion

18 system required for mycobacterial pathogenesis (1, 2). Previous studies revealed that mycobac-

19 terial strains lacking the outer lipid PDIM have impaired ESX-1 function during laboratory growth

20 and infection (3-5). The mechanisms underlying changes in ESX-1 function are unknown. We

21 used a proteo-genetic approach to measure PDIM and PGL-dependent protein secretion in *M.*

22 *marinum,* a non-tubercular mycobacterial pathogen that causes tuberculosis-like disease in ec-

23 tothermic animals (6, 7). Importantly, *M. marinum* is a well-established model for mycobacterial

24 pathogenesis (8, 9). Our findings showed that *M. marinum* strains without PDIM and PGL

25   showed specific, significant reductions in protein secretion compared to the WT and comple-

26   mented strains. We recently established a hierarchy for the secretion of ESX-1 substrates in

27   four (I-IV) groups (10). Loss of PDIM differentially impacted secretion of Groups III and IV ESX-

28   1 substrates, which are likely the effectors of pathogenesis. Our data suggests that the altered

29   secretion of specific ESX-1 substrates is responsible for the observed ESX-1-related effects in

30   PDIM-deficient strains.

31

32   **Importance:** *Mycobacterium tuberculosis,* the cause of human tuberculosis, killed an estimated

33   1.3 million people in 2022. Non-tubercular mycobacterial species are causing acute and chronic

34   human infections. Understanding how these bacteria cause disease is critical. Lipids in the cell

35   envelope are essential for mycobacteria to interact with the host and promote disease. Strains

36   lacking outer lipids are attenuated for infection, but the reasons are unclear. Our research aims

37   to identify a mechanism for attenuation of mycobacterial strains without the PDIM and PGL

38   outer lipids in *M. marinum.* These findings will enhance our understanding of the importance of

39   lipids in pathogenesis, and how these lipids contribute to other established virulence mecha-

40   nisms.

41   **Introduction:**

42   Phthiocerol dimycocerosate (PDIM) and phenolic glycolipid (PGL) are outer lipid virulence fac-

43   tors in the mycolate outer membrane (MOM) (11-13). Although the precise role of PDIM/PGL in

44   mycobacterial virulence remains elusive, PDIM/PGL support cell envelope structure, serve as a

45   permeability barrier, enhance antibiotic tolerance, and directly modulate the immune system

46   (14-18). These lipids recruit macrophages permissive for bacterial growth and survival while

47   promoting evasion of bactericidal macrophages (11, 13, 17, 19-22).

48   PDIM and PGL are synthesized from cytoplasmic fatty acids via a series of discrete

49   steps by the PpsA-E/FadD26, Mas/FadD28 and PapA5 enzymes (23-25). Their transport across

50 the cytoplasmic membrane (CM) and mycobacterial arabinogalactan peptidoglycan complex

51 (mAGP) relies on the MmpL7 and DrrABC transporters, and the LppX lipoprotein (11, 13, 26-

52 29), although the precise mechanisms remain unknown.

53   Mycobacteria secrete proteins across the MOM to the cell surface and into the surround-

54 ing environment both during laboratory growth and infection (30-34). Proteins are exported

55 across the CM by the Sec and SecA2 pathways, twin arginine transporter (TAT), and ESAT-6

56 (ESX) systems (35, 36). Yet, the mechanisms used by proteins to cross the impermeable

57 mAGP and the MOM (37-39) are elusive. Recent studies suggest that PE/PPE and Esx

58 (WXG_100) proteins facilitate protein translocation across the MOM (10, 40, 41).

59   Early during infection, mycobacterial secreted proteins promote interaction with host

60 membranes and macrophage signaling pathways. The ESX-1 system secretes proteins that

61 contribute to phagosomal damage (42-44), leading to pathogen release, along with its DNA,

62 RNA and secreted proteins, into the macrophage cytoplasm (22, 44-46). Secreted proteins in

63 the cytoplasm hinder phagosomal repair, affect host trafficking and promote dissemination of

64 infected macrophages in the lung (44, 47-52). Mycobacterial DNA in the cytoplasm triggers the

65 Type I IFN response (43, 45, 46, 53), promoting macrophage cell death and bacterial spread

66 (43, 54).

67   In the absence of PDIM, ESX-1 function is reduced, affecting the Type I IFN response

68 and phagosomal lysis (3, 4). It is unclear whether PDIM is required for ESX-1 protein secretion

69 across the MOM (3) or for ESX-1 substrate function within the phagosome (4). Our study uses a

70 proteogenetic approach (55) to quantify how PDIM and PGL influence protein secretion from

71 *Mycobacterium marinum*. Our studies provide an explanation for the ESX-1 phenotypes in the

72 absence of PDIM, suggesting a broader role of PDIM and PGL outer lipids in translocating my-

73 cobacterial proteins across the MOM.

74 **Results:**

75   **Generation and characterization of PDIM deficient *M. marinum* strains.** The PDIM/PGL bi-

76   osynthetic pathway is conserved in both *M. tuberculosis* and *M. marinum* (Figure 1A). We previ-

77   ously constructed *M. marinum* strains with disrupted PDIM production due to deletion of the *mas*

78   gene (56) or the second ER domain of the *ppsC* gene (57). We generated an *M. marinum* strain

79   with an unmarked deletion of the *drrABC* genes. PpsA-E/FadD26 synthesize phthiocerol; loss of

80   the PpsCER domain ablates activity and abrogates PDIM production (19, 57-59). Mas/FadD28

81   synthesize mycocerosic acid; deletion of *mas* halts PDIM production (12, 23). The two PDIM

82   components are joined by PapA5 and transported by DrrABC, MmpL7 and LppX (12, 25-27).

83   Deletion of *drrABC* abolishes PDIM production and transport (12). Complementation strains

84   were generated by introducing integrating plasmids with the $ppsC_{ER}$ domain, the *drrABC* operon

85   or the *mas* gene behind constitutive promoters into each deletion strain. We confirmed the re-

86   sulting strains using PCR (Fig. S1) followed by targeted DNA sequencing, and qRT-PCR to

87   measure transcription in the deletion and complementation strains (Fig. 1B and Fig. S2A and B).

88   Deletion of the *mas* or *drrABC* genes abolished expression relative to the WT and complement-

89   ed strains. Deletion of the $ppsC_{ER}$ domain did not impact *ppsC* expression, as expected (57).

90   We validated PDIM and PGL loss in each deletion strain (Fig. 1C and Fig. S2C) by iso-

91   lating total soluble lipids and visualizing PDIM and PGL using thin layer chromatography. All

92   three *M. marinum* deletion strains exhibited a lack of PDIM and PGL (Fig. 1C and Fig S2C). Re-

93   introducing the *mas* gene restored PDIM in the Δ*mas* strain (Fig. 1C). PDIM and PGL were not

94   complemented by restoring gene expression in the Δ$ppsC_{ER}$ and Δ*drrABC* strains (Fig. S2C).

95

96   **The loss of PDIM/PGL has a general effect on mycobacterial protein secretion.**

97   Past studies linked ESX-1 secretion and PDIM/PGL, proposing that PDIM is necessary

98   for ESX-1 protein secretion (3). To clarify PDIM/PGL's role in mycobacterial protein secretion,

99   we isolated secreted and cell associated protein fractions and quantified the protein levels in the

100   mutant and complemented strains compared to the WT *M. marinum* strain using Label Free

101   Quantitative (LFQ) Proteomics (Dataset S1). We measured ESX-1-dependent protein secretion

102   as a control.

103   Deletion of the *eccCb₁* gene reduced ESX-1 substrate production and secretion (Fig. 2,

104   top)*. We reasoned that if PDIM was specifically required for ESX-1 secretion, then deletion of

105   the *mas, ppsC_{ER}* or *drrABC* genes will abolish ESX-1 secretion, similar to the Δ*eccCb₁* strain.

106   Deletion of the *mas* gene (or deletion of the *drrABC* genes or the ER domain from the *ppsC*

107   gene) resulted in a significant decrease in the levels of most secreted proteins (Fig. 2, middle

108   and Fig. S3). Restoring *mas* expression in the Δ*mas* strain complemented the secretion defect

109   (Fig. 2, bottom). These data support that PDIM is important for overall protein secretion from *M.*

110   *marinum* during laboratory growth.

111

112   **The loss of PDIM/PGL specifically impacts the secretion of a subset of ESX-1 substrates.**

113   We previously demonstrated that ESX-1 substrates are hierarchically secreted from *M.*

114   *marinum.* We categorized them into at least four groups of ESX-1 substrates (Fig. 3A, (10)).

115   Group 1 includes EsxA, EsxB, PPE68 and MMAR_2894, which are essential for the secretion of

116   the other ESX-1 substrates (10, 60, 61). Group 2 substrates include EspB, EspJ and EspK (10,

117   60, 62). These substrates are not required for the secretion of Group 1 substrates, but are es-

118   sential for the secretion of ESX-1 Group 2 substrates (10). ESX-1 Group 3 substrates include

119   EspE and EspF, and these substrates are dispensable for the secretion of the other ESX-1 sub-

120   strate classes. Importantly, deletion of the Group 3 substrates is sufficient to abrogate the he-

121   molytic activity of *M. marinum* (63).

122   Figure 3B and 3C indicates that the loss of PDIM specifically impacts the secretion of

123   ESX-1 Group 3 substrates. In the Δ*eccCb₁* strain, ESX-1 substrate levels were significantly re-

124   duced (Figure S4, Dataset S1) due to feedback control of substrate gene transcription in the

125   absence of the ESX-1 system (64). However, in the Δ*mas* strain, the substrate levels were not

126 significantly reduced (Fig. S4), indicating no feedback control of substrate gene transcription

127 due to the loss of the PDIM/PGL lipids. While ESX-1 substrate secretion was significantly re-

128 duced from the Δ*eccCb₁* strain because EccCb₁ is directly required for substrate secretion (1,

129 65, 66), the levels of ESX-1 substrates secreted from the Δ*mas* strain differed, aligning with

130 previously established substrate groups (Fig. 3B and C, Dataset S1). The Group 3 substrates

131 (EspE, EspF) were the most affected by PDIM/PGL loss. The reduced secretion of Group 3

132 substrates were complemented by expression of *mas* in the Δ*mas* strain (Fig. 3B and 3C). To-

133 gether, these data support that the loss of PDIM/ PGL differentially impacts the secretion of the

134 known ESX-1 substrates.

135

136 **The absence of PDIM reduces ESX-1 function.**

137 Prior research demonstrated that PDIM-deficient *M. marinum* strain exhibited lower

138 ESX-1-dependent hemolytic activity (5). EspE and EspF secretion were most impacted by

139 PDIM/PGL loss. Deleting *espE* or *espF* from *M. marinum* abrogated hemolytic activity and at-

140 tenuated *M. marinum* during macrophage infection (63). Because deleting *espE* or *espF* did not

141 significantly affect the secretion of the additional known ESX-1 substrates, EspE and EspF are

142 at the top of the hierarchy (10). In Figure 4A, WT *M. marinum* lysed sheep red blood cells

143 (sRBCs) in a contact dependent, ESX-1 dependent manner. The Δ*eccCb₁* strain which lacks

144 ESX-1 secretion, had significantly less hemolytic activity than the WT strain ($P<.0001$) (10, 61,

145 63). The Δ*mas* strain exhibited intermediate hemolytic activity, between the WT ($P<.0001$) and

146 Δ*eccCb₁* strains ($P<.0001$), similar to a prior report (5). Reintroducing the *mas* gene in the Δ*mas*

147 strain significantly increased hemolysis ($P<.0001$), but not to WT levels (WT vs Δ*mas*/p*mas*,

148 $P<.0001$).

149 We next used western blot analysis to examine ESX-1 substrate secretion. EsxB (CFP-

150 10) was made (Fig. 4B, lane 1) and secreted (lane 4) from the WT strain. EsxB production was

151 reduced (lane 2) and it was not secreted (lane 6) from the Δ*eccCb₁* strain, as previously report-

152   ed (57). EsxB production (lanes 3 and 4) and secretion (lanes 7 and 8) were not noticeably im-

153   pacted in the Δ*mas* and Δ*mas* complemented strains. EspE was produced (lane 1) and secret-

154   ed (lane 5) from the WT strain. EspE levels were reduced in (lane 2) and was not secreted from

155   the Δ*eccCb$_1$* strain (lane 6). Although EspE was made to WT levels in the Δ*mas* strain (lane 3),

156   EspE secretion was reduced (lane 7). EspE secretion was restored in Δ*mas*/p*mas* strain (lane

157   8). These data are consistent with the LFQ proteomics data in Figures 2 and 3. Interestingly, as

158   we replicated the western blot analysis, we sometimes observed no visible secretion phenotype,

159   as shown in Figure 4, right. The LFQ analysis did not reveal WT levels of EspE and EspF in any

160   of the replicates we tested. From these data, we conclude that western blot analysis, which is

161   not quantitative, may lack the sensitivity to detect intermediate but biologically relevant changes

162   in ESX-1 protein secretion, as supported by our prior work (10, 60).

163

164   **Discussion:**

165   This study aimed to understand the impact of the outer lipids PDIM and PGL on ESX-1 secre-

166   tion. We measured a broad and significant reduction in *M. marinum* protein secretion in the ab-

167   sence of PDIM and PGLs. Interestingly, the loss of PDIM and PGLs differentially impacted ESX-

168   1 protein secretion, particularly affecting the secretion of the Group 3 substrates, EspE and

169   EspF. Our findings support that the ESX-1-associated phenotypes in strains lacking PDIM/ PGL

170   are due to the reduced secretion of specific ESX-1 substrates.

171   At least three publications previously linked PDIM to ESX-1 secretion or function (3-5).

172   Barczak et al. concluded PDIM is required for ESX-1 substrate secretion in *M. tuberculosis*. De-

173   letion of *drrC* abrogated EsxA (ESAT-6) and EsxB (CFP-10) secretion, and the ESX-5 sub-

174   strate, EspN, during laboratory growth. Other PDIM deficient strains in this study had WT-levels

175   of EsxB secretion. The loss of ESX-1 secretion led to reduced IFN induction during macrophage

176   infection with the Δ*drrC* strain as compared to the WT and complemented strains. IFN induction

177 requires ESX-1 induced lysis of the phagosome membrane (44, 53). They concluded that the

178 PDIM lipid at the cell surface was important for ESX-mediated protein secretion (3).

179 In Barczak et al. an intermediate secretion signal may have been missed because the

180 amount of protein loaded in that study was based on the culture density as measured by

181 OD_{600}(3). We normalized the protein levels based on protein concentration as measured by

182 BCA assay, because the OD_{600} of *M. marinum* grown Sauton's media with low Tween-80 is an

183 unreliable measure in our hands. Using this approach, we did not observe significant differences

184 in the secretion of the Group 1 substrates, which includes EsxB, by western blot analysis or us-

185 ing LFQ proteomics. Importantly, Barczak et al. observed variability in EsxB secretion by differ-

186 ent PDIM deficient strains (Δ*drrC* vs Δ*drrA*). Our study revealed that reduced EspE secretion

187 was variable when detected by western blot analysis, but not by proteomics. We think the in-

188 consistency in measuring these secretory phenotypes by western blot likely stems from their

189 intermediate nature.

190 Quigley et al. connected PDIM transport to ESX-1 dependent events during macrophage

191 infection, including phagosome lysis and the resulting macrophage cell death (4). They showed

192 significantly reduced phagosomal lysis of an Δ*mmpL7 M. tuberculosis* strain compared to the

193 WT and complemented strains. Aligned with our studies, Quigley et al. loaded 10μg of protein,

194 found no defect in EsxA secretion by western blot analysis.

195 Osman et al. demonstrated that PDIM transport was important for phagosomal lysis,

196 finding reduced phagosomal lysis of an Δ*mmpL7 M. marinum* strain during macrophage infec-

197 tion (5). Although the Δ*mmpL7* strain exhibited intermediate hemolytic activity between the

198 ΔRD1 and WT strains, their data did not meet statistical significance. They suggested that PDIM

199 enhanced the ESX-1 lytic activity, but offered that PDIM may contribute differently to hemolysis

200 and phagosomal lysis. Our results show that *M. marinum* strains lacking PDIM/PGL production

201 (Δ*mas* or Δ*ppsC*) or transport (Δ*drrABC*) have significantly reduced hemolysis compared the

202 WT strain, and significantly higher hemolysis compared to the Δ*eccCb$_1$ M. marinum* strain. We

203   assessed hemolysis 90 minutes after initiating contact between *M. marinum* and the sRBCs,

204   while Osman et al measured hemolysis after two hours (5). We previously found intermediate

205   hemolysis phenotypes are most apparent at earlier timepoints (64, 67). We suspect that the in-

206   termediate hemolytic activity of the Δ*mmpL7* strain would have reached significance relative to

207   WT strain at earlier timepoints.

208   An underlying commonality in all of these studies is that in strains lacking PDIM or PGL,

209   ESX-1 activity is reduced, as reflected in hemolytic activity or phagosomal lysis during infection.

210   Notably, at the time of these manuscripts, the secretory relationship between ESX-1 substrates

211   was unclear. However, we now know that EspE/EspF secretion is essential for hemolysis, and

212   for pathogenesis in macrophages (63). We have likewise defined a hierarchical secretory rela-

213   tionship between the ESX-1 substrates (10). Here we showed that the loss of PDIM specifically

214   reduced EspE/EspF secretion from *M. marinum*. Therefore, we hypothesize that reduced Es-

215   pE/EspF secretion caused the reduced hemolytic and phagolytic activity observed in the ab-

216   sence of PDIM. It is tempting to speculate that the secretion of proteins that colocalize with

217   PDIM and PGL in the mycobacterial envelope is impacted by the loss of these lipids in *M. mari-*

218   *num*. This idea requires further exploration beyond these initial studies.

219   Our unbiased approach to measuring protein secretion revealed that losing PDIM/PGL

220   broadly impacts protein secretion. Contrary to expectations based on PDIM's role in maintaining

221   envelope impermeability, making the cell envelope permeable did not increase protein secretion

222   by increasing cellular lysis. Instead, overall protein secretion in the culture supernatants de-

223   creased, despite evidence of cellular lysis. Our study has direct implications for mycobacterial

224   pathogenesis, as PDIM and PGL deficient *Mycobacterium* are attenuated in cellular infection

225   models (11, 13, 58). Further study is needed to understand if the observed phenotypes due to

226   the loss of mycobacterial outer lipids stem from changes in the secreted proteome.

227

228   **Methods:**

229 **Growth of Bacterial Strains:** *Mycobacterium marinum* strains were derived from *Mycobacte-*

230 *rium marinum* M strain (ATCC BAA-535). *M. marinum* strains were maintained at 30°C in either

231 Middlebrook 7H9 Broth Base (Sigma Aldrich) supplemented with 0.5% glycerol and 0.1%

232 Tween-80 (Fisher Scientific) or Middlebrook 7H11 Agar (Sigma Aldrich) plates supplemented

233 with 0.5% glucose and 0.5% glycerol. Where appropriate, strains were supplemented with 50

234 µg/mL hygromycin B (Corning, Corning, NY), 20 µg/mL kanamycin (IBI Scientific, Dubuque, IA),

235 and 60 µg/mL X-Gal (RPI, Mount Prospect, IL). *Escherichia coli* DH5α strains were grown in Lu-

236 ria-Bertani Broth (VWR) at 37°C and supplemented with 200 µg/mL hygromycin and 50 µg/mL

237 kanamycin, where appropriate.

238
239 **Construction of *M. marinum* strains:** The *ΔdrrABC* strain was generated using allelic ex-

240 change using the p2NIL vector [Addgene plasmid number 20188; a gift from Tanya Parish (68)]

241 and the pGOAL19 vector [Addgene plasmid number 20190; a gift from Tanya Parish (68)], as

242 previously published (61, 63, 64, 67, 69). Primers were purchased from Integrated DNA Tech-

243 nologies (IDT, Coralville, IA) and are listed in Table S2. The complementation plasmids were

244 generated using FastCloning (70) using *M. marinum* M genomic DNA. Plasmids were intro-

245 duced into *M. marinum* using electroporation as described previously (61, 63, 64, 67, 69, 71).

246 Strains and plasmids are listed in Supplementary Tables S1. Plasmids and genetic deletions

247 were confirmed by targeted DNA sequencing performed by the Notre Dame Genomics and Bio-

248 informatics Facility.

249
250 **Thin-Layer Chromatography of PDIM and PGL Lipids:** 5 mL cultures of *M. marinum* in 7H9

251 defined broth (Millipore Sigma), and grown for 2-3 days until turbid, diluted into 50mL of 7H9

252 defined broth to an OD_{600} of 0.05 and grown for 72 hours. Mycobacterial cells were harvested via

253 centrifugation (4000 rpm for 10 minutes). The resulting cell pellets were washed three times with

254 phosphate-buffered saline (PBS). Lipids were extracted using a chloroform (Ricca Chemical

255 Company, Arlington, TX) :methanol (Millipore Sigma) mixture (2:1) overnight in a fume hood.

256 Overnight extraction mixtures were filtered through 6 mm Whatman filter paper (Millipore Sigma)

257 using a porcelain Buchner funnel before separating aqueous and organic phase layers. Extract-

258 ed lipids were moved to a clean glass vial and dried overnight in a fume hood under a gentle

259 stream of air. Dried mycobacterial lipids were resuspended in a 100 µl mixture of chloroform:

260 methanol (2:1) prior to analysis.

261 9 µl of total mycobacterial lipids were spotted onto aluminum-backed silica TLC plates

262 (Millipore Sigma) and dried. To separate mycobacterial phthiocerol dimycocerosates (PDIM)

263 and triacylglycerols (TAG), spotted lipids were migrated three times sequentially in a running

264 solution of 50:1 petroleum ether (Sigma Aldrich) and ethyl acetate (Sigma Aldrich). The TLC

265 plate was sprayed with phosphomolybdic acid (Millipore Sigma) and charred via heat gun

266 (Westward) to visualize lipids.

267 Mycobacterial phenolic glycolipids (PGLs) were visualized using 9µl of total mycobacte-

268 rial lipids migrated once in a solution of 96:4 chloroform and methanol. The TLC plate was

269 sprayed with a solution of 1% α-naphthol (TCI Chemicals, Portland, OR) and charred via heat

270 gun to visualize lipids.

271

272 **Hemolysis Assays:** Hemolysis assays were performed exactly as described (10) except that

273 sheep red blood cell and bacteria were incubated at 30°C for one and a half hours, rather than

274 two hours.

275

276 **Secretion Assays:** Cell-associated and secreted protein fractions were prepared from *M. mari-*

277 *num* exactly as previously described (10). Briefly, *M. marinum* bacterial cultures were grown in

278 7H9 defined media, diluted into 50 mL of Sauton's media at an OD_{600} of 0.8 and grown for 48

279 hours before harvesting cellular and secreted fractions by centrifugation. Culture supernatants

280 were filtered through 0.2 µm Nalgene Rapid-Flow Bottle Top Filters with PES membranes

281 (Thermo Scientific) and concentrated using 15 mL, 3kDa Amicon Ultra Centrifugal Filter Units

282 (Millipore Sigma). Mycobacterial cell pellets were resuspended in 0.5 mL of PBS, lysed via

283 bead-beating with a BioSpec Mini-Beadbeater-24, and clarified by centrifugation. Protein con-

284 centrations of the resulting fractions were measured Pierce Micro BCA Protein Assay Kit (Ther-

285 mo Scientific).

286

287 **Western Blot Analysis:** 10 µg of each protein sample was loaded into 4-20% TGX Gradient

288 Gels (Bio-Rad) for analysis. Antibodies were diluted in 5% non-fat dry milk (RPI) in PBS with

289 0.1% Tween-20 (VWR). Rpoβ (anti-RNA polymerase beta mouse monoclonal antibody [clone:

290 8RB13]; VWR) was diluted 1:20,000. The following reagents were obtained through BEI re-

291 sources, NIAID, NIH: polyclonal anti-*Mycobacterium tuberculosis* CFP-10 (gene Rv3874; antise-

292 rum, rabbit; NR-13801) and polyclonal anti-*Mycobacterium tuberculosis* Mpt-32 (gene Rv1860;

293 antiserum, rabbit; NR-13807). CFP-10 was used at a 1:5,000 dilution. Mpt-32 was used at a

294 1:30,000 dilution. The EspE antibody (1:5,000 dilution) was a custom rabbit polyclonal antibody

295 against the CGQQATLVSDKKEDD peptide (Genscript).

296

297 **Proteomics/LC-MS:** LC-MS pure reagents (water, ethanol, acetonitrile, and methanol) were

298 purchased from J.T. Baker (Radnor, PA). Iodoacetamide (IAA) was purchased from MP Bio-

299 medicals (Solon. OH). All other reagents are from Sigma-Aldrich (St. Louis, MO) unless speci-

300 fied. S-Trap mini devices were from Protifi (Huntington, NY). Trypsin Gold was purchased from

301 Promega (Madison, WI). Hydrophilic–lipophilic balance (HLB) solid phase extraction (SPE) car-

302 tridges (1 cc/10 mg) from Waters (Milford, MA) were used to desalt peptide samples prior to

303 analysis on a timsTOF Pro from Bruker Scientific LLC (Billerica, MA). Protein and peptide iden-

304 tification including label-free quantitation was performed using the PEAKS Online X search en-

305 gine from Bioinformatics Solutions Inc (Waterloo, ON) (build 1.4.2020-10-21_171258).

306   Cell-associated and secreted cell lysate samples were prepared for LC-MS analysis as

307 described (72, 73). 50 µg of each sample was prepared in 100 mM triethylammonium bicar-

308   bonate (TEAB), 5% sodium dodecyl sulfate (SDS), and 100 mM tris(2-carboxyethyl)phosphine

309   (TCEP). Samples were heated for 10 minutes at 95˚C, cooled, then IAA was added to 100 mM

310   IAA for 30 minutes in dark.

311   Samples were acidified with *o*-phosphoric acid to a final concentration of 1.2% in 50 µL,

312   then flocculated with 350 µL Binding Buffer containing 90% methanol and 10% 1M TEAB. Sam-

313   ples were passed through S-Trap Micro filters and followed by two 80 µL washes of Binding

314   Buffer and 80 µL of 1:1 methanol/chloroform solution. A new collection tube was added, and 1

315   µg of trypsin in 80 µL was added. Samples were wrapped in Parafilm to prevent evaporative

316   loss and incubated at 37˚C for 12 hours. Digested peptides were spun through the filter, fol-

317   lowed by two 80 µL elutions with 0.1% formic acid in water, and one 80 µL elution with 0.1%

318   formic acid in 50% acetonitrile. Eluted peptides were vacuum concentrated for 20 minutes (to

319   remove acetonitrile), and then desalted using 1cc/10 mg HLB SPE cartridges following manu-

320   facturer's specifications, and dried by vacuum concentrator prior to analysis.

321   Desalted peptides were resuspended in 0.1% formic acid and water, to 1 mg/mL con-

322   centration. 100 ng of each sample was injected in triplicate onto an Evosep One and timsTOF

323   Pro LC-MS system. Each sample was prepared in biological triplicate and technical triplicate.

324   15spd (Sample-per-day) methods were used on a 150 µm x 150 mm PepSep column with C_{18}

325   ReproSil AQ stationary phase at 1.9mm particle size, 120Å pore size (Manufacturer's protocol).

326   Samples were loaded using Evotips following manufacturer's specifications. Nano-ESI was

327   used with a spray voltage of 1700V. MS was set to Parallel Accumulation, Serial Fragmentation

328   Data Dependent Mode (PASEF-DDA) with a mass range of 100–1700 m/z, ion mobility range of

329   0.6–1.6 v*s/cm^2, and ramp and accumulation times of 100 ms. Each precursor consisted of 10

330   PASEF ramps for a cycle time of 1.17 s. Precursors were filtered to contain only charges from 2

331   to 5. MS/MS collision energy settings were set to ramp from 20 eV at 0.6 ion mobility to 70 eV at

332   1.6 ion mobility. Instrument tune parameters were set to default for proteomic studies with the

333 following differences: quadrupole low mass set to 20 m/z, focus pre-TOF pre-pulse storage set

334 to 5 ms.

335 Protein and peptide identification and label-free quantitation were performed using the

336 PEAKS Online X search engine. Search database used was the *M. marinum* proteome from

337 Mycobrowser (v4 release). Search settings were set to manufacturer defaults unless specified.

338 3 missed cleavages were allowed, at a semi-specific search. Fixed modification included car-

339 bamidomethylation of cysteine, while variable modifications included protein N-terminal acetyla-

340 tion, deamidation of asparagine and glutamine, pyroglutamic acid from glutamine and glutamic

341 acid, and oxidation of methionine. All peptide-spectrum matches were filtered to a 1% false dis-

342 covery rate. Cell-associated samples were normalized by total ion current (TIC). RAW files are

343 deposited and available at MassIVE/Proteome Exchange

344 ftp://MSV000093713@massive.ucsd.edu (password PDIM2024#) MSV000093713.

345 LFQ search results were trimmed as follows. Technical replicate values for each sample

346 were averaged if at least two of the three replicates were nonzero values. The same averaging

347 logic was applied to biological replicates. Only nonzero values were averaged. All mutant sam-

348 ples were ratioed the corresponding WT values, to generate fold-change ratios.

349 **RNA extraction:** *M. marinum* strains were grown as described in the Secretion Assays meth-

350 ods section. 15 mL of Sauton's culture were pelleted by centrifugation. Bacterial pellets were

351 resuspended in Qiagen RLT buffer (Qiagen, Hilden, Germany) supplemented with 1% β-

352 mercaptoethanol. Lysates were generated by bead beating with the Biospec Mini-BeadBeater-

353 24 and clarified with centrifugation. Total RNA was extracted using the RNeasy Mini Kit (Qi-

354 agen), according to manufacturer's instructions.

355 **qRT-PCR:** RNA (500 ng) was treated with RQ1 DNase (Promega) according to the manufactur-

356 er's instructions. 1 µl of DNase treated RNA was converted to cDNA using random hexamers

357 (IDT) and SuperScript II Reverse Transcriptase (Invitrogen) according to manufacturer instruc-

358 tions. cDNA was quantified using a Nanodrop 2000 (Thermo Scientific, Waltham, MA). 10 μl

359 qRT-PCR reactions were prepped with 250 ng of cDNA, SYBR^{TM} Green PCR Master Mix (Ap-

360 plied Biosystems, Carlsbad, CA) and 1 μM of each oligonucleotide. Reactions were run using

361 Applied Biosystems MicroAmp Fast 96-well plates (0.1 ml) (Life Technologies). Plates were run

362 on QuantStudio 3 Real-Time PCR system (Thermo Fisher). Cycle conditions were as follows:

363 50 °C for 2 min., 95 °C for 10 min. then 40 cycles at 95 °C for 15 sec and 60 °C for 1 min. Then,

364 a dissociation step of 95 °C for 15 sec., 60 °C for 1 min., 95 °C for 15 sec., and 60 °C for 15

365 sec.

366 qRT-PCR reactions were analyzed using ΔΔCt comparisons. qRT-PCR results were

367 normalized to WT transcript abundance using the following equations:

368

369 $$\Delta Ct = Ct(\text{gene of interest}) - Ct(\text{housekeeping gene})$$

370 Then:

371 $$\Delta\Delta Ct = \Delta Ct(\text{treated sample}) - \Delta Ct(\text{untreated sample})$$

372 Then:

373 $$2^{-\Delta\Delta Ct} = \text{fold change}$$

374

375 **R Code for Volcano Plots:**

376 >WT_vs_dmas$threshold=as.factor(WT_vs_dmas$Significance < 13)
377 *Determine which Proteins were significantly changed, 13 is the 95% percentile or 10$^{-1.3}$*

378 > g <- ggplot(data = WT_vs_dmas, aes(x=L2FC, y = Significance, color = threshold)) + ge-
379 om_point(alpha = 0.4, size = 1.75) + xlim(c(-8, 8)) + xlab("log2 fold change") + (ylab("-log10 p-
380 value")+ theme_bw() + theme(legend.position = "none"))
381 > g
382 > g +theme(text=element_text(size = 20))+ geom_hline(yintercept = -log10(0.05), linetype =
383 "dashed")   +   geom_vline(xintercept = c(log2(0.5), log2(2)), linetype =
384 "dashed")+scale_x_continuous(breaks = c(seq(-8,8,2)))
385

References

1. S. A. Stanley, S. Raghavan, W. W. Hwang, J. S. Cox, Acute infection and macrophage subversion by Mycobacterium tuberculosis require a specialized secretion system. *Proc Natl Acad Sci U S A* **100**, 13001-13006 (2003).

2. T. Hsu *et al.*, The primary mechanism of attenuation of bacillus Calmette-Guerin is a loss of secreted lytic function required for invasion of lung interstitial tissue. *Proc Natl Acad Sci U S A* **100**, 12420-12425 (2003).

3. A. K. Barczak *et al.*, Systematic, multiparametric analysis of Mycobacterium tuberculosis intracellular infection offers insight into coordinated virulence. *PLoS Pathog* **13**, e1006363 (2017).

4. J. Quigley *et al.*, The Cell Wall Lipid PDIM Contributes to Phagosomal Escape and Host Cell Exit of Mycobacterium tuberculosis. *MBio* **8** (2017).

5. M. M. Osman, A. J. Pagan, J. K. Shanahan, L. Ramakrishnan, Mycobacterium marinum phthiocerol dimycocerosates enhance macrophage phagosomal permeabilization and membrane damage. *PLoS One* **15**, e0233252 (2020).

6. F. Linell, A. Norden, Mycobacterium balnei, a new acid-fast bacillus occurring in swimming pools and capable of producing skin lesions in humans. *Acta Tuberc Scand Suppl* **33**, 1-84 (1954).

7. H. F. Clark, C. C. Shepard, Effect of Environmental Temperatures on Infection with Mycobacterium Marinum (Balnei) of Mice and a Number of Poikilothermic Species. *J Bacteriol* **86**, 1057-1069 (1963).

8. T. C. Pozos, L. Ramakrishnan, New models for the study of Mycobacterium-host interactions. *Curr Opin Immunol* **16**, 499-505 (2004).

9. A. E. Chirakos, A. Balaram, W. Conrad, P. A. Champion, Modeling Tubercular ESX-1 Secretion Using Mycobacterium marinum. *Microbiol Mol Biol Rev* **84** (2020).

10. R. M. Cronin, M. J. Ferrell, C. W. Cahir, M. M. Champion, P. A. Champion, Proteogenetic analysis reveals clear hierarchy of ESX-1 secretion in Mycobacterium marinum. *Proc Natl Acad Sci U S A* **119**, e2123100119 (2022).

11. L. R. Camacho, D. Ensergueix, E. Perez, B. Gicquel, C. Guilhot, Identification of a virulence gene cluster of Mycobacterium tuberculosis by signature-tagged transposon mutagenesis. *Mol Microbiol* **34**, 257-267 (1999).

12. L. R. Camacho *et al.*, Analysis of the phthiocerol dimycocerosate locus of Mycobacterium tuberculosis. Evidence that this lipid is involved in the cell wall permeability barrier. *J Biol Chem* **276**, 19845-19854 (2001).

13. J. S. Cox, B. Chen, M. McNeil, W. R. Jacobs, Jr., Complex lipid determines tissue-specific replication of Mycobacterium tuberculosis in mice. *Nature* **402**, 79-83 (1999).

14. A. M. Block *et al.*, Mycobacterium tuberculosis Requires the Outer Membrane Lipid Phthiocerol Dimycocerosate for Starvation-Induced Antibiotic Tolerance. *mSystems* **8**, e0069922 (2023).

15. M. S. Siegrist, C. R. Bertozzi, Mycobacterial lipid logic. *Cell Host Microbe* **15**, 1-2 (2014).

16. S. A. Stanley, J. S. Cox, Host-Pathogen Interactions During Mycobacterium tuberculosis infections. *Curr Top Microbiol Immunol* **374**, 211-241 (2013).

17. C. J. Cambier *et al.*, Mycobacteria manipulate macrophage recruitment through coordinated use of membrane lipids. *Nature* **505**, 218-222 (2014).

18. C. Passemar *et al.*, Multiple deletions in the polyketide synthase gene repertoire of Mycobacterium tuberculosis reveal functional overlap of cell envelope lipids in host-pathogen interactions. *Cell Microbiol* **16**, 195-213 (2014).

19. C. J. Cambier, S. M. O'Leary, M. P. O'Sullivan, J. Keane, L. Ramakrishnan, Phenolic Glycolipid Facilitates Mycobacterial Escape from Microbicidal Tissue-Resident Macrophages. *Immunity* **47**, 552-565 e554 (2017).

20. M. A. Kirksey *et al.*, Spontaneous phthiocerol dimycocerosate-deficient variants of Mycobacterium tuberculosis are susceptible to gamma interferon-mediated immunity. *Infect Immun* **79**, 2829-2838 (2011).

21. T. A. Day *et al.*, Mycobacterium tuberculosis strains lacking surface lipid phthiocerol dimycocerosate are susceptible to killing by an early innate host response. *Infect Immun* **82**, 5214-5222 (2014).

22. Y. Cheng, J. S. Schorey, Mycobacterium tuberculosis-induced IFN-beta production requires cytosolic DNA and RNA sensing pathways. *J Exp Med* **215**, 2919-2935 (2018).

23. A. K. Azad, T. D. Sirakova, L. M. Rogers, P. E. Kolattukudy, Targeted replacement of the mycocerosic acid synthase gene in Mycobacterium bovis BCG produces a mutant that lacks mycosides. *Proc Natl Acad Sci U S A* **93**, 4787-4792 (1996).

24. A. K. Azad, T. D. Sirakova, N. D. Fernandes, P. E. Kolattukudy, Gene knockout reveals a novel gene cluster for the synthesis of a class of cell wall lipids unique to pathogenic mycobacteria. *J Biol Chem* **272**, 16741-16745 (1997).

25. O. A. Trivedi *et al.*, Dissecting the mechanism and assembly of a complex virulence mycobacterial lipid. *Mol Cell* **17**, 631-643 (2005).

26. M. Jain, J. S. Cox, Interaction between polyketide synthase and transporter suggests coupled synthesis and export of virulence lipid in M. tuberculosis. *PLoS Pathog* **1**, e2 (2005).

27. G. Sulzenbacher *et al.*, LppX is a lipoprotein required for the translocation of phthiocerol dimycocerosates to the surface of Mycobacterium tuberculosis. *EMBO J* **25**, 1436-1444 (2006).

28. M. H. Touchette, J. C. Seeliger, Transport of outer membrane lipids in mycobacteria. *Biochim Biophys Acta* 10.1016/j.bbalip.2017.01.005 (2017).

29. M. H. Touchette *et al.*, A Screen for Protein-Protein Interactions in Live Mycobacteria Reveals a Functional Link between the Virulence-Associated Lipid Transporter LprG and the Mycolyltransferase Antigen 85A. *ACS Infect Dis* **3**, 336-348 (2017).

30. C. Abou-Zeid *et al.*, The secreted antigens of Mycobacterium tuberculosis and their relationship to those recognized by the available antibodies. *J Gen Microbiol* **134**, 531-538 (1988).

31. M. G. Sonnenberg, J. T. Belisle, Definition of Mycobacterium tuberculosis culture filtrate proteins by two-dimensional polyacrylamide gel electrophoresis, N-terminal amino acid sequencing, and electrospray mass spectrometry. *Infect Immun* **65**, 4515-4524 (1997).

32. Y. Ge *et al.*, Top down characterization of secreted proteins from Mycobacterium tuberculosis by electron capture dissociation mass spectrometry. *J Am Soc Mass Spectrom* **14**, 253-261 (2003).

33. E. F. Perkowski *et al.*, The EXIT Strategy: an Approach for Identifying Bacterial Proteins Exported during Host Infection. *MBio* **8** (2017).

34. F. Sayes *et al.*, Multiplexed Quantitation of Intraphagocyte Mycobacterium tuberculosis Secreted Protein Effectors. *Cell Rep* **23**, 1072-1084 (2018).

35. L. S. Ligon, J. D. Hayden, M. Braunstein, The ins and outs of Mycobacterium tuberculosis protein export. *Tuberculosis (Edinb)* **92**, 121-132 (2012).

36. C. Chagnot, M. A. Zorgani, T. Astruc, M. Desvaux, Proteinaceous determinants of surface colonization in bacteria: bacterial adhesion and biofilm formation from a protein secretion perspective. *Front Microbiol* **4**, 303 (2013).

37. P. A. Lambert, Cellular impermeability and uptake of biocides and antibiotics in Gram-positive bacteria and mycobacteria. *J Appl Microbiol* **92 Suppl**, 46S-54S (2002).

38. A. H. Delcour, Outer membrane permeability and antibiotic resistance. *Biochim Biophys Acta* **1794**, 808-816 (2009).

39. P. S. Manzanillo *et al.*, The ubiquitin ligase parkin mediates resistance to intracellular pathogens. *Nature* **501**, 512-516 (2013).

40. L. S. Ates *et al.*, Essential Role of the ESX-5 Secretion System in Outer Membrane Permeability of Pathogenic Mycobacteria. *PLoS Genet* **11**, e1005190 (2015).

41. Q. Wang *et al.*, PE/PPE proteins mediate nutrient transport across the outer membrane of Mycobacterium tuberculosis. *Science* **367**, 1147-1151 (2020).

42. N. van der Wel *et al.*, M. tuberculosis and M. leprae translocate from the phagolysosome to the cytosol in myeloid cells. *Cell* **129**, 1287-1298 (2007).

43. R. Simeone *et al.*, Phagosomal rupture by Mycobacterium tuberculosis results in toxicity and host cell death. *PLoS Pathog* **8**, e1002507 (2012).

44. D. Houben *et al.*, ESX-1-mediated translocation to the cytosol controls virulence of mycobacteria. *Cell Microbiol* **14**, 1287-1298 (2012).

45. P. S. Manzanillo, M. U. Shiloh, D. A. Portnoy, J. S. Cox, Mycobacterium Tuberculosis Activates the DNA-Dependent Cytosolic Surveillance Pathway within Macrophages. *Cell Host Microbe* **11**, 469-480 (2012).

46. R. O. Watson, P. S. Manzanillo, J. S. Cox, Extracellular M. tuberculosis DNA Targets Bacteria for Autophagy by Activating the Host DNA-Sensing Pathway. *Cell* **150**, 803-815 (2012).

47. A. Coros, B. Callahan, E. Battaglioli, K. M. Derbyshire, The specialized secretory apparatus ESX-1 is essential for DNA transfer in Mycobacterium smegmatis. *Mol Microbiol* **69**, 794-808 (2008).

48. M. S. Siegrist *et al.*, Mycobacterial Esx-3 is required for mycobactin-mediated iron acquisition. *Proc Natl Acad Sci U S A* **106**, 18792-18797 (2009).

49. S. R. Elliott, A. D. Tischler, Phosphate responsive regulation provides insights for ESX-5 function in Mycobacterium tuberculosis. *Curr Genet* **62**, 759-763 (2016).

50. T. A. Gray *et al.*, Intercellular communication and conjugation are mediated by ESX secretion systems in mycobacteria. *Science* **354**, 347-350 (2016).

51. C. Portal-Celhay *et al.*, Mycobacterium tuberculosis EsxH inhibits ESCRT-dependent CD4(+) T-cell activation. *Nat Microbiol* **2**, 16232 (2016).

52. E. Mittal *et al.*, Mycobacterium tuberculosis Type VII Secretion System Effectors Differentially Impact the ESCRT Endomembrane Damage Response. *MBio* **9**, e01765-01718 (2018).

53. S. A. Stanley, J. E. Johndrow, P. Manzanillo, J. S. Cox, The Type I IFN response to infection with Mycobacterium tuberculosis requires ESX-1-mediated secretion and contributes to pathogenesis. *J Immunol* **178**, 3143-3152 (2007).

54. D. G. Russell, The ins and outs of the Mycobacterium tuberculosis-containing vacuole. *Cell Microbiol* **18**, 1065-1069 (2016).

55. K. R. Nicholson, C. B. Mousseau, M. M. Champion, P. A. Champion, The genetic proteome: Using genetics to inform the proteome of mycobacterial pathogens. *PLoS Pathog* **17**, e1009124 (2021).

56. O. A. Collars *et al.*, An N-acetyltransferase required for ESAT-6 N-terminal acetylation and virulence in Mycobacterium marinum. *mBio* **14**, e0098723 (2023).

57. E. A. Williams *et al.*, A Nonsense Mutation in Mycobacterium marinum That Is Suppressible by a Novel Mechanism. *Infect Immun* **85** (2017).

58. J. Yu *et al.*, Both phthiocerol dimycocerosates and phenolic glycolipids are required for virulence of Mycobacterium marinum. *Infect Immun* **80**, 1381-1389 (2012).

59. O. Vergnolle *et al.*, Biosynthesis of cell envelope-associated phenolic glycolipids in Mycobacterium marinum. *J Bacteriol* **197**, 1040-1050 (2015).

60. M. M. Champion, E. A. Williams, R. S. Pinapati, P. A. Champion, Correlation of Phenotypic Profiles Using Targeted Proteomics Identifies Mycobacterial Esx-1 Substrates. *J Proteome Res* **3**, 5151-5164 (2014).

61. R. E. Bosserman, K. R. Nicholson, M. M. Champion, P. A. Champion, A New ESX-1 Substrate in Mycobacterium marinum That Is Required for Hemolysis but Not Host Cell Lysis. *J Bacteriol* **201** (2019).

62. B. McLaughlin *et al.*, A mycobacterium ESX-1-secreted virulence factor with unique requirements for export. *PLoS Pathog* **3**, e105 (2007).

63. A. E. Chirakos, K. R. Nicholson, A. Huffman, P. A. Champion, Conserved ESX-1 substrates EspE and EspF are virulence factors that regulate gene expression. *Infect Immun* 10.1128/IAI.00289-20 (2020).

64. R. E. Bosserman *et al.*, WhiB6 regulation of ESX-1 gene expression is controlled by a negative feedback loop in Mycobacterium marinum. *Proc Natl Acad Sci U S A* 10.1073/pnas.1710167114 (2017).

65. K. M. Guinn *et al.*, Individual RD1-region genes are required for export of ESAT-6/CFP-10 and for virulence of Mycobacterium tuberculosis. *Mol Microbiol* **51**, 359-370 (2004).

66. L. Y. Gao *et al.*, A mycobacterial virulence gene cluster extending RD1 is required for cytolysis, bacterial spreading and ESAT-6 secretion. *Mol Microbiol* **53**, 1677-1693 (2004).

67. K. G. Sanchez *et al.*, EspM Is a Conserved Transcription Factor That Regulates Gene Expression in Response to the ESX-1 System. *mBio* **11** (2020).

68. T. Parish, N. G. Stoker, Use of a flexible cassette method to generate a double unmarked Mycobacterium tuberculosis tlyA plcABC mutant by gene replacement. *Microbiology* **146 (Pt 8)**, 1969-1975 (2000).

69. R. E. Bosserman, C. R. Thompson, K. R. Nicholson, P. A. Champion, Esx Paralogs Are Functionally Equivalent to ESX-1 Proteins but Are Dispensable for Virulence in Mycobacterium marinum. *J Bacteriol* **200**, e00726-00717 (2018).

70. C. Li *et al.*, FastCloning: a highly simplified, purification-free, sequence- and ligation-independent PCR cloning method. *BMC Biotechnol* **11**, 92 (2011).

71. T. Parish, Electroporation of Mycobacteria. *Methods Mol Biol* **2314**, 273-284 (2021).

72. J. W. Saelens *et al.*, An ancestral mycobacterial effector promotes dissemination of infection. *Cell* https://doi.org/10.1016/j.cell.2022.10.019 (2022).

575   73.   O. A. Collars *et al.*, An N-acetyltransferase required for EsxA N-terminal protein
576   acetylation   and   virulence   in   Mycobacterium   marinum.   *bioRxiv*
577   10.1101/2023.03.14.532585, 2023.2003.2014.532585 (2023).
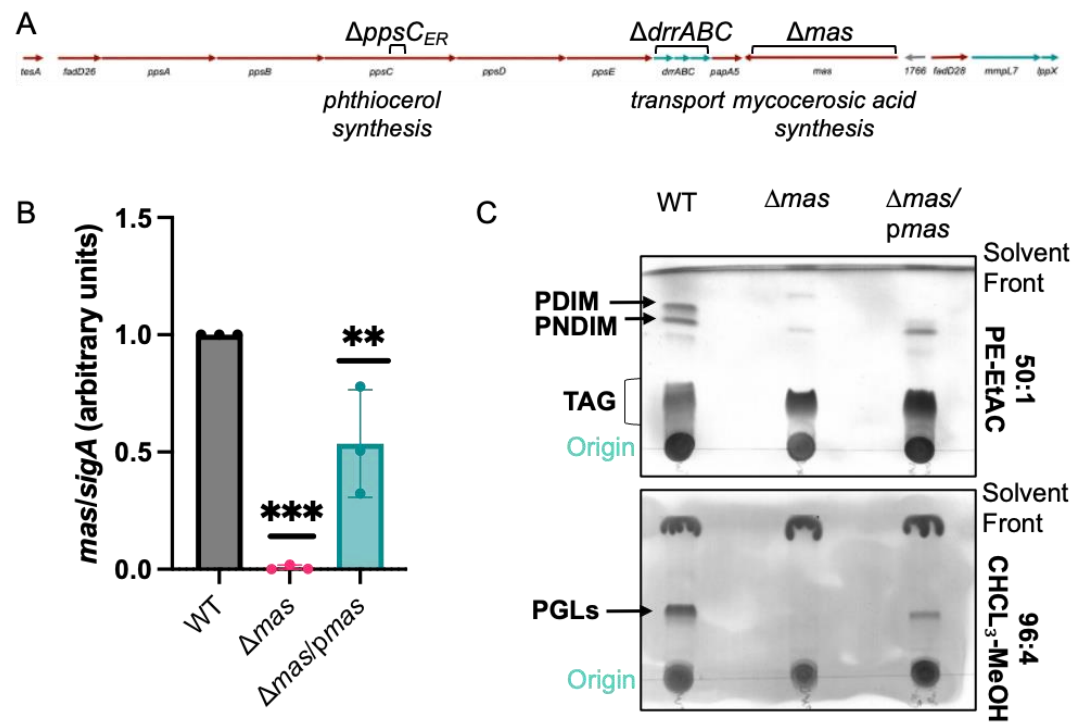578

579

Figures and Legends:

Figure 1. Characterization of PDIM/PGL deficient _M. marinum_ strains. A. Schematic of the genetic loci required for PDIM production and transport. B. qRT-PCR of _mas_ transcript relative to the _sigA_ transcript compared to the WT _M. marinum_ strain. Each datapoint is an independent biological replicate, and an average of three technical replicates. Statistical analysis was performed using an ordinary one-way ANOVA (P=.0003), followed by a Dunnett's multiple comparison test, *** P=.0002, ** P=.0093. C. TLC of total lipids isolated from the WT, Δ_mas_ and complemented _M. marinum_ strains. 9 μl of total lipids was analyzed. This TLC is representative of at least three independent biological replicates.
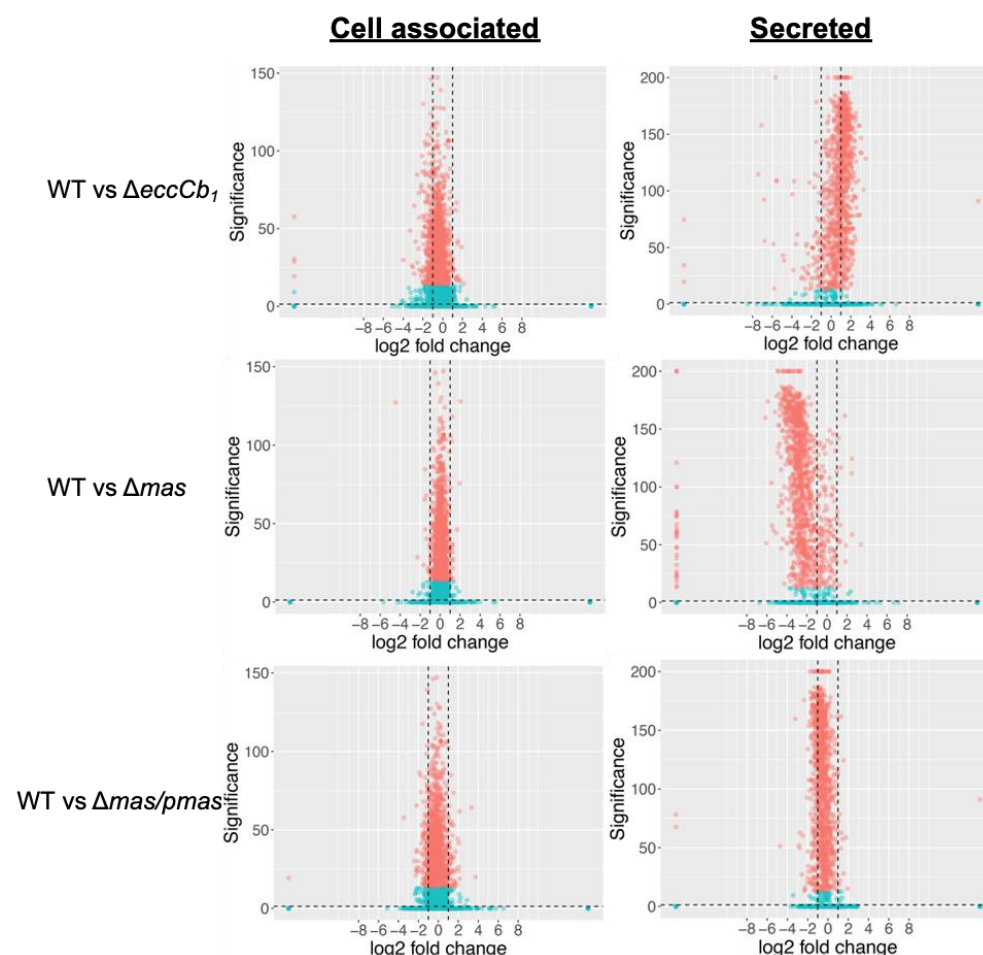
Figure 2. Loss of PDIM/ PGL results in widespread changes to protein secretion from *M. marinum.* Volcano plots of the secreted protein levels from cell associated (left) and secreted protein fractions from *M. marinum.* Values are the average of four biological replicates. Significance was plotted against the log2 fold change compared to the WT strain. blue dots indicate *P* ≤ 0.05; red dots indicate *P* > 0.05. Vertical, black dashed lines signify a log2 foldchange = +/- 1.
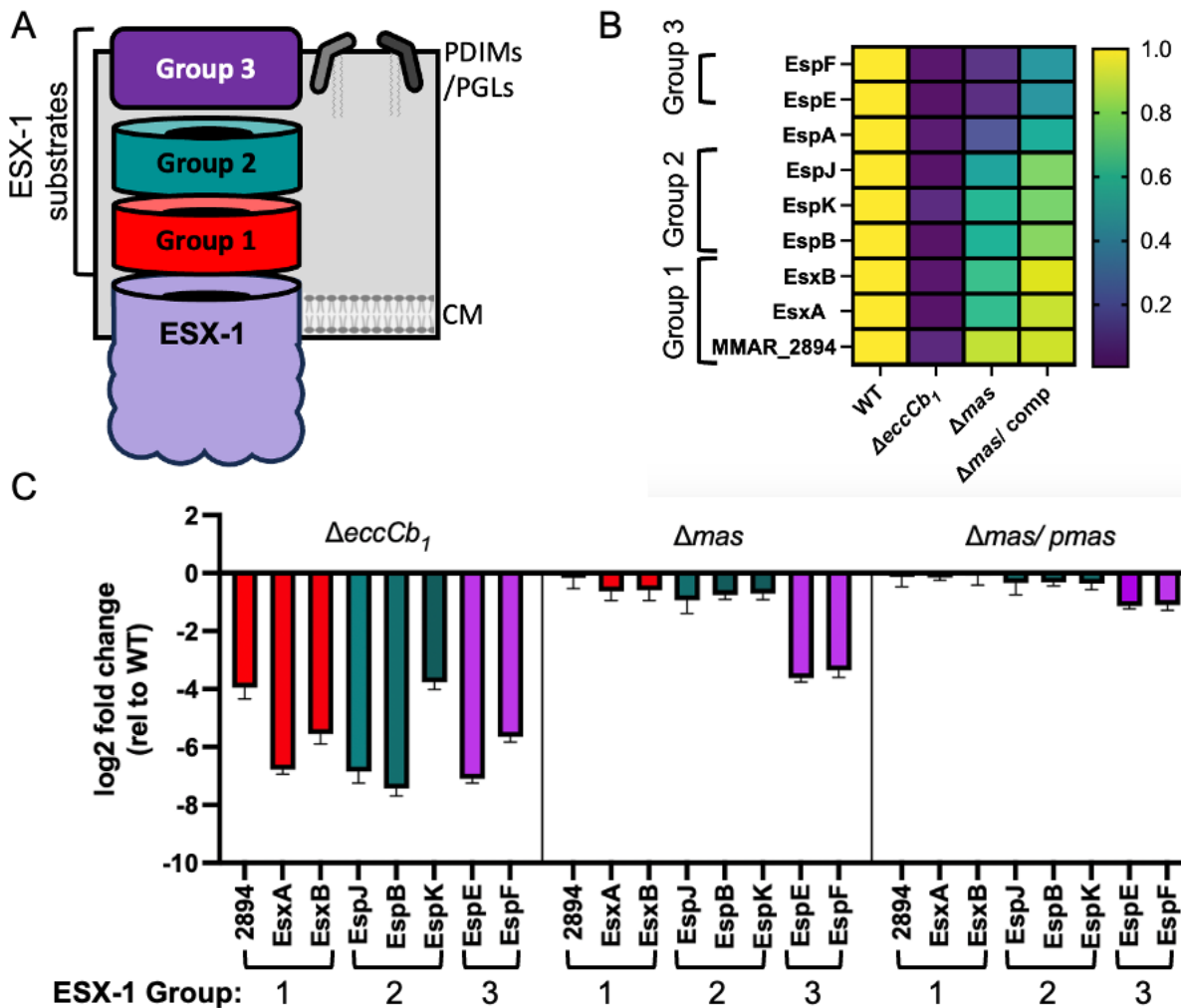
602

Figure 3. The loss of PDIM/PGL impacts ESX-1 secretion differentially. A. Schematic of the ESX-1 secretion hierarchy. ESX-1 represents the ESX-1 membrane components. Group 1: EsxB, EsxA, PPE68 and MMAR_2894, Group 2: EspB, EspK, EspJ, Group 3: EspE and EspF, from (10). **B.** Log2 Fold-Change of ESX-1 substrate levels in the secreted protein fractions compared to the WT strain. Data in Dataset 1C. **C.** Heat map of the ESX-1 substrate levels in the secreted protein fractions normalized to the WT strains (Data in Dataset 1D, from Dataset S1B)
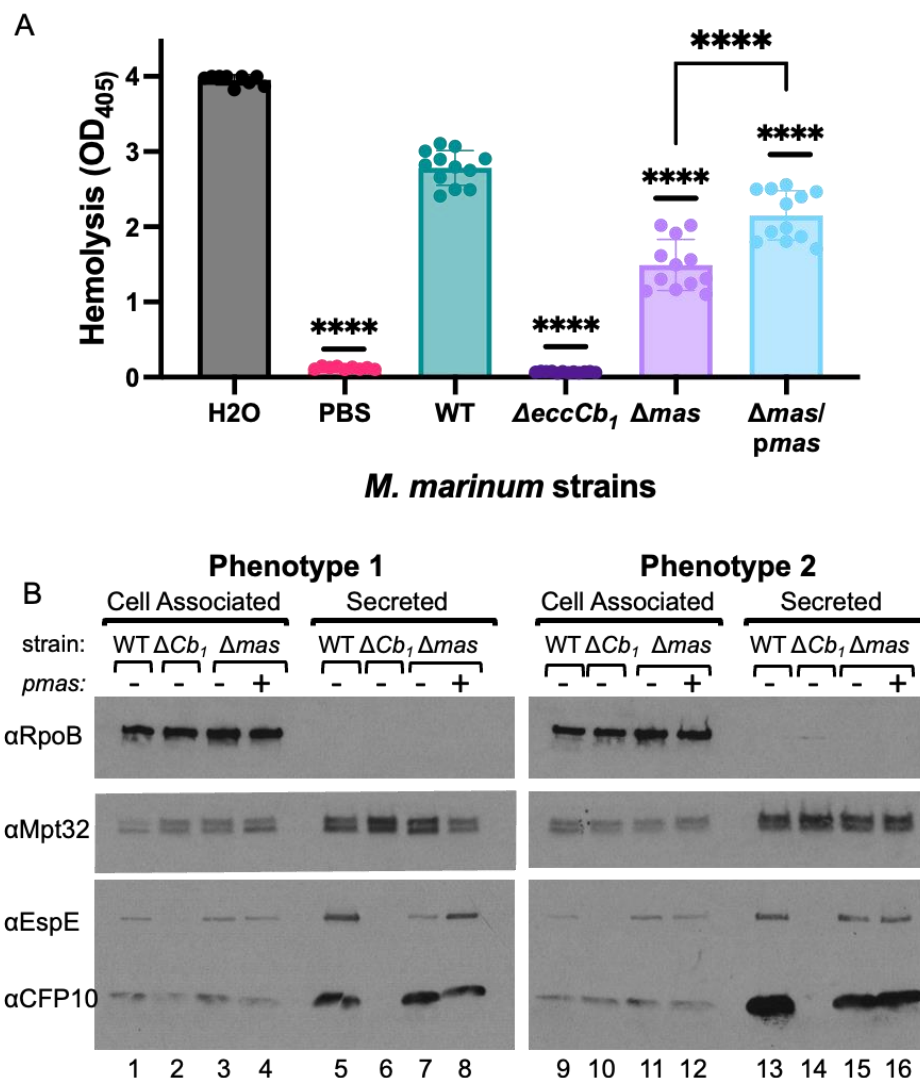
610

Figure 4. The loss of PDIM/PGL impacts hemolysis and the secretion of the EspE substrate. A. Hemolytic activity of *M. marinum.* Each data point is a single technical replicate, making up four biological replicates. Significance was determined using a one-way ANOVA, $P<.0001$, followed by a Tukey's multiple comparison test **** $P<.0001$. **B.** Western blot analysis of *M. marinum* cell associated and secreted protein fractions. 10 μg of protein were loaded in each lane. RpoB is a control for lysis, MPT32, a protein secreted by the Sec system, is a loading control. The two blots shown were representative of at least four biological replicates.